

Topic	Identification and analysis of short-period core phases (tutorial with exercise by hand)
Authors	Peter Bormann (formerly GFZ German Research Centre for Geosciences, D-14473 Potsdam, Germany); E-mail: pb65@gmx.net Siegfried Wendt , Universität of Leipzig, Institut für Geophysik und Geologie, Geophysikalisches Observatorium Collm, D-04779 Wernsdorf, Germany, E-mail: wendt@rz.uni-leipzig.de
Version	June 2002; DOI: 10.2312/GFZ.NMSOP-2_EX_11.3

1 Aim

This manual exercise aims at making you familiar with the identification of both direct and multiple-reflected longitudinal core phases and their use in location and magnitude determination. Clear short-period vertical component PKP seismograms of a single station contain all information needed to determine *source depth* h , *epicentral distance* D and *magnitude* m_b with an accuracy of ± 30 km, better $\pm 1.5^\circ$ and ± 0.3 magnitude units, respectively. In case of strong seismic sources and the availability of identically calibrated horizontal components with good signal-to-noise ratio, additionally the backazimuth to the source can be determined with an accuracy of about $\pm 5^\circ$ - 10° and thus the approximate location. Additionally, the identification of late reflected core phases and their use in distance determination is practiced. These phases are very suitable for calculating the epicentral distance since their relative travel-time difference to the related first arrival P or PKP is nearly independent of source depth.

2 Data

- Figure 1: Compilation of typical analog short-period recordings at station MOX, Germany, of the different direct core phases from earthquakes between $135^\circ < D < 160^\circ$;
- Figure 2: Plots of digital broadband records of the German Regional Seismograph Network (GRSN), filtered according to a WWSSN-SP response, from a Fiji-Island earthquake within the distance range 148.4° (CLL) to 152.2° (BFO);
- Figure 3: Three record examples with PKPab, bc and df phases to be analyzed;
- Figure 4: Four records with later longitudinal core phases to be evaluated;
- Figure 5: Travel times and paths of the direct longitudinal core phases and their relationship to the P-wave velocity model of the Earth;
- Figure 6: Ray path of the reflected core phases P'P' (or PKPPKP) and PKKP;
- Figure 7: Differential travel-time curves pPKP-PKP for $D = 150^\circ$;
- Figure 8: Differential travel-time curves PKPbc-PKPdf (PKP1-PKIKP) and PKPab-PKPdf (PKP2-PKIKP);
- Figure 9: Differential travel-time curves PKKP-P and PKKP-PKP, respectively;
- Figure 10: Differential travel-time curves PKPPKP-P.
- Figure 11: Record with identified onsets.
- Figure 12: Magnitude calibration functions for PKPdf (old PKIKP), PKPbc (old PKP1) and PKPab (old PKP2).

Note 1: All differential travel-time curves given in this exercise have been calculated according to the earth model IASP91 (Kennett and Engdahl, 1991). The more recent model AK135 (Kennett et al., 1995) yields still better travel-times for core phases. The difference, however, is more significant for absolute and usually negligible for differential travel times.

Note 2: The first record example in Figure 1 illustrates that at $D < 145^\circ$ small amplitude precursors PKPpre of waves scattered from the core-mantle boundary (CMB) may occur. In the case of crustal earthquakes PKPdif may additionally be followed closely by depth phases. Together this may mimic a core phase triplication typical for $D > 146^\circ$. Yet, in the case of deep earthquakes with sharp onsets and no or small signal coda, the triple group of phases is usually rather distinct and its typical pattern easily recognizable.

Note 3: The typical three-phase pattern PKPdif (alternative name PKIKP), PKPbc (old name PKP1) and PKPab (old name PKP2) is however well developed between $146^\circ < D < 155^\circ$ only. Around 145° all three phases arrive at the same time and thus superpose to a rather strong impulsive onset.

Note 4: Beyond 154° still a weak intermediate phase between PKPdif and PKPab may be observed up to about 160° along the extrapolation of the PKPbc travel-time branch. It is, however, not PKPbc proper but rather the phase PKPdif which is diffracted around the inner-core boundary (see last record example in Figure 1).

Note 5: In the last record example of Figure 1 the well developed depth phase obviously relates to the strongest direct phase PKPab (old PKP2). The depth phases pPKP may, in the case of maximum possible source depth around 700 km, follow the related direct phases after up to about 2.5 minutes. When the primary core phases are rather strong, two or three related depth phases may be discernable.

Note 6: More examples based on plots from digital seismic records are given in DS 11.3.

Additionally, for the magnitude determinations, measured trace amplitudes have to be converted into ground motion amplitudes. For this the frequency dependent amplitude-magnification of the seismograph has to be known. It is given in Table 1.

Table 1 Magnification MAG of ground displacement in the seismic records of earthquakes No. 1, 2 and 3 in Figure 3 when these are reproduced with a time scale of 1 mm/s.

Period (in s)	0.9	1.0	1.1	1.2	1.3	1.4	1.6	1.8	2.0	2.4
MAG Event 1		52,440		49,210		44,090	37,550	30,660	24,420	14,000
MAG Event 2		26,220		24,600		22,040	18,770	15,330	12,210	7,000
MAG Event 3	62,020	56,000	49,980	43,960	37,940					

3 Procedure

All steps of determining h , D , AZI and mb will be practiced.

Source depth and **epicentral distance** are determined by reading the relative onset-time difference in seconds or minutes, respectively, between identified phases and using the corresponding differential travel-time curves. Note that these curves in Figures 7 and 8 have been presented with the same time-resolution as the analog records in Figure 3, i.e. with 1

mm/s. If a transparent overlay is produced from these curves, the source depth and the epicentral distance, respectively, from the records depicted in Figure 3 can be directly determined by matching the related curves with the identified onsets. Make sure that the depth and distance axes, respectively, are kept perpendicular to the center line of the record trace when matching. When reading the time differences PKKP-P and P'P'-P in Figure 4 be aware, that the time difference between subsequent traces from top to bottom is 15 minutes. Full minutes start at the left side of the 2 second long gaps or „faintings“ on the record traces.

The **backazimuth** is determined according to the instructions given under 3.2 in EX 11.2.

For epicenter **location** based on the estimated epicentral distance D and the backazimuth AZI one may use either a sufficiently large globe (diameter about 0.5 to 1 m), mark there the position of the considered station and then use a bendable ruler with the same scale in degree as your globe and an azimuth dial to find the source location on the globe. Another possibility is to use a global map projection which shows isolines of equal backazimuth and distance from your station (as Figure 5 in EX 11.2). Such maps can nowadays easily be calculated and plotted by means of computers.

The **magnitude $mb(\text{PKP})$** is determined according to an experimental calibration function for magnitude determinations based on short-period readings of various PKP phases in the distance range 145° to 164° . It has been developed by S. Wendt (Bormann and Wendt, 1999). Its world-wide testing is recommended. The following relationship is used:

$$mb(\text{PKP}) = \log_{10} (A/T) + Q(\Delta, h)_{\text{PKP}} \quad (1)$$

with amplitude A in μm (10^{-6} m). If more than one PKP phase PKPab, PKPbc and/or PKPdf can be identified and A and T been measured then the individual phase magnitudes should be determined first and then the average magnitude be calculated. The latter provides a more stable estimate.

4 Tasks

- 4.1 Train yourself first by matching the travel-time curve overlay of Figure 8 with the onsets marked in Figure 1, taking into account the distance and focal depth given for each earthquake. Also consult Figure 2 and the related notes 1 to 6 in section Data above. Then mark on the records in Figure 3 for all three earthquakes the onset times of recognizable phases and give them names, both for the early and the late arrivals (depth phases).
- 4.2 Measure the time difference pPKP-PKP for the strongest PKP arrival and its respective depth phase and determine the source depth for all three earthquakes by using the differential travel-time curves given in Figure 7. Note: If the pPKP group is less distinct and its different onsets can not be well separated then relate the depth phase to the strongest direct PKP arrival.
- 4.3 Determine the epicentral distance D (in $^\circ$) of the three earthquakes shown in Figure 3 by using the differential travel-time curves shown in Figure 8 taking into account for each event the source depth determined under 4.2.

- 4.4 Measure the time difference between the P-wave first arrivals and the PKKP or P'P' phases marked in the four records presented and determine the epicentral distance D for these earthquakes by using the differential travel-time curves shown in Figures 9 and 10, respectively.
- 4.5 Estimate from the three-component record in Figure 3 (event No. 3) for the strongest phase the backazimuth AZI according to relationship and instructions given under 3.2 of EX 11.2.
- 4.6 Try to find for event No. 3, which had been recorded at the station CLL in Germany, the source location on the map shown in Figure 5 of EX 11.2. Give the name of the source area.
- 4.7 Measure the trace amplitudes B (in mm) and related periods T for all identified phases of direct PKP in Figure 3 and convert them into "true ground motion" amplitudes A (in nm) by means of Table 1 given above in section Data.
- 4.8 Determine $\log(A/T)$ and estimate the related values for $\sigma(D, h)$ from Figure 12. Note that these values are valid for amplitudes in μm only! Correct them for nm.
- 4.9 Give the individual magnitude estimates for PKPab, PKPbc and PKPdf,
- 4.10 Calculate the average $\bar{m}_b(\text{PKP})$.
- 4.11 Compare your results with the respective solutions given by the NEIC for these three earthquakes and assess the achievable accuracy of respective individual source parameter calculations at single stations, even when based on analog recordings only and simple analysis tools.

5 Solutions

5.1 See Figure 11.

5.2 NEIC gave for the three earthquakes the following hypocentral depths:

- | | |
|-------|----------------------|
| No. 1 | $h = 435 \text{ km}$ |
| No. 2 | $h = 235 \text{ km}$ |
| No. 3 | $h = 540 \text{ km}$ |

Your own depth estimates should be within about $\pm 30 \text{ km}$ of these values. But this does not mean that your value is worse than that given by NEIC. It may be even better, because NEIC mostly does not use depth phases to constrain its solutions from direct P-wave readings.

5.3 NEIC calculated for the stations which recorded the three earthquakes in Figure 3 the following epicentral distances $\Delta = D$ (in $^\circ$):

- | | |
|-------|-------------------|
| No. 1 | $D = 148.5^\circ$ |
| No. 2 | $D = 159.5^\circ$ |
| No. 3 | $D = 150.3^\circ$ |

Using the recommended travel-time curves, your estimates should be within $\pm 1.5^\circ$ of these values.

5.4 NEIC calculated for the station CLL which had recorded the earthquakes shown in Figure 4 the following epicentral distances:

- No. 1 $D = 98.5^\circ$
 No. 2 $D = 111.2^\circ$
 No. 3 $D = 66.3^\circ$
 No. 4 $D = 57.3^\circ$

Using the recommended travel-time curves, your estimates should be within $\pm 1.5^\circ$ to NEIC.

5.5 $AZI \approx 22^\circ$. Your own estimate should be within $\pm 5^\circ$ of this value.

5.6 Fiji Islands

5.7 Event No. 1: PKPdf	$B = 0.5 \text{ mm}, T = 1.5 \text{ s} \rightarrow A = 12.2 \text{ nm}$
PKPbc	$B = 3.9 \text{ mm}, T = 1.0 \text{ s} \rightarrow A = 74.4 \text{ nm}$
PKPab	$B = 3.0 \text{ mm}, T = 1.0 \text{ s} \rightarrow A = 57.2 \text{ nm}$
Event No. 2: PKPdf	$B = 2.9 \text{ mm}, T = 2.4 \text{ s} \rightarrow A = 414.3 \text{ nm}$
PKPab	$B = 8.2 \text{ mm}, T = 2.0 \text{ s} \rightarrow A = 671.6 \text{ nm}$
Event No. 3: PKPdf	$B = 0.95 \text{ mm}, T = 1.3 \text{ s} \rightarrow A = 21.6 \text{ nm}$
PKPbc	$B = 20.4 \text{ mm}, T = 1.0 \text{ s} \rightarrow A = 329.0 \text{ nm}$
PKPab	$B = 6.5 \text{ mm}, T = 1.0 \text{ s} \rightarrow A = 116.1 \text{ nm}$

5.8 Event No. 1: PKPdf	$\log(A/T) = 0.9$	$\sigma_{\text{PKPdf}}(\Delta, h) = 3.95$
PKPbc	$\log(A/T) = 1.89$	$\sigma_{\text{PKPbc}}(\Delta, h) = 3.15$
PKPab	$\log(A/T) = 1.76$	$\sigma_{\text{PKPab}}(\Delta, h) = 3.39$
Event No. 2: PKPdf	$\log(A/T) = 2.24$	$\sigma_{\text{PKPdf}}(\Delta, h) = 3.8$
PKPab	$\log(A/T) = 2.53$	$\sigma_{\text{PKPab}}(\Delta, h) = 3.55$
Event No. 3: PKPdf	$\log(A/T) = 1.22$	$\sigma_{\text{PKPdf}}(\Delta, h) = 3.94$
PKPbc	$\log(A/T) = 2.52$	$\sigma_{\text{PKPbc}}(\Delta, h) = 3.23$
PKPab	$\log(A/T) = 2.06$	$\sigma_{\text{PKPab}}(\Delta, h) = 3.55$

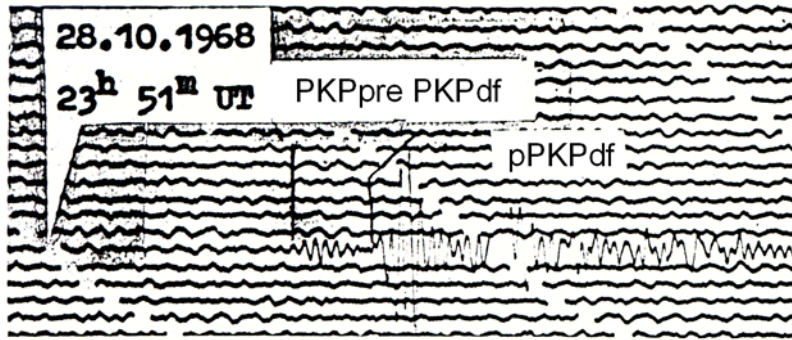
5.9 Event No. 1: $mb(\text{PKPdf}) = 4.85$; $mb(\text{PKPbc}) = 5.04$; $mb(\text{PKPab}) = 5.15 \rightarrow \overline{mb}(\text{PKP}) = 5.0$
 Event No. 2: $mb(\text{PKPdf}) = 6.0$; $mb(\text{PKPab}) = 6.1 \rightarrow \overline{mb}(\text{PKP}) = 6.0$
 Event No. 3: $mb(\text{PKPdf}) = 5.19$; $mb(\text{PKPbc}) = 5.75$; $mb(\text{PKPab}) = 5.61 \rightarrow \overline{mb}(\text{PKP}) = 5.5$

5.10 NEIC gave for these three events, based on teleseismic P-wave readings only:

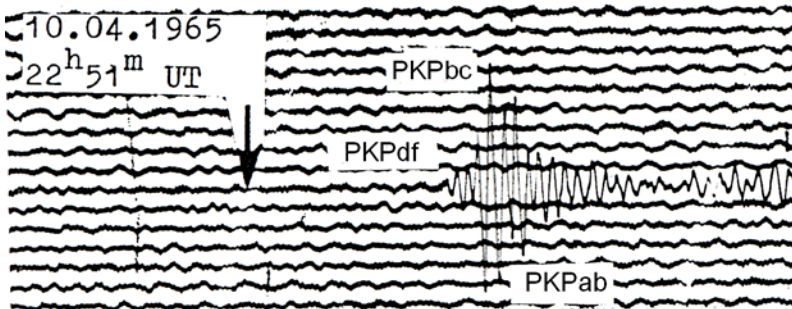
- Event No. 1: $mb = 5.0$,
 Event No. 2: $mb = 5.5$,
 Event No. 3: $mb = 5.3$

5.11 Using the calibration curves for PKP waves one can get quick mb estimates from readings of PKP amplitudes at individual stations with simple analysis tools which are within about ± 0.5 magnitudes units to the mb estimates of global seismological services. Your distance estimates should also be within $\pm 1.5^\circ$ even when using only low-resolution analog data and visual time picks. The general source area can be determined properly, even for very

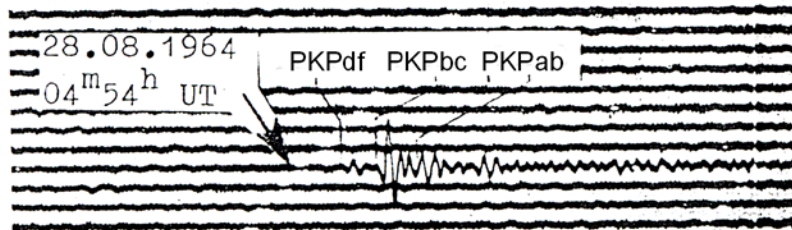
distant events, on the basis of properly mutually calibrated 3-component recordings of single seismic stations.



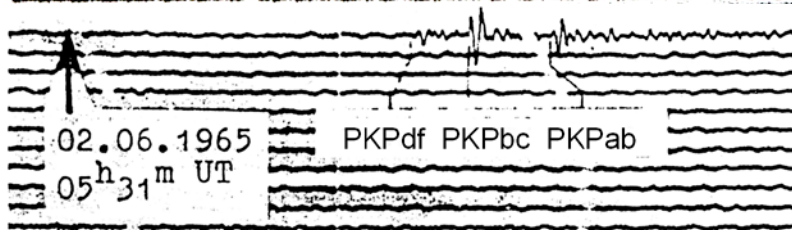
$D = 135.5^\circ$
 $h = 60 \text{ km}$
 $mb = 5.9$
 Santa Cruz Islands



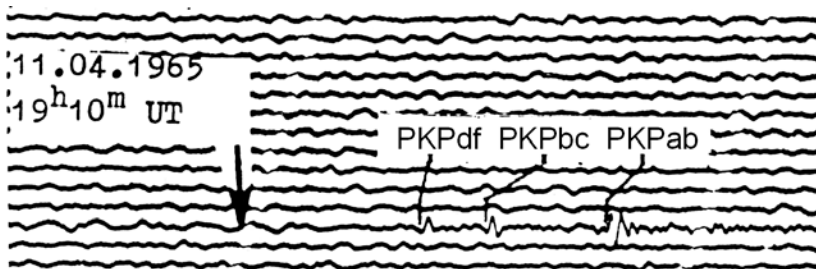
$D = 146.7^\circ$
 $h = 543 \text{ km}$
 $mb = 5.9$
 Fiji Islands



$D = 148.3^\circ$
 $h = 580 \text{ km}$
 $mb = 5.4$
 Fiji Islands



$D = 151.3^\circ$
 $h = 539 \text{ km}$
 $mb = 5.6$
 Fiji Islands



$D = 153.6^\circ$
 $h = 581 \text{ km}$
 $mb = 5.5$
 South of Fiji Islands

$D = 159.5^\circ$, $h = 231 \text{ km}$
 $mb = 5.5$, Kermadec Islands

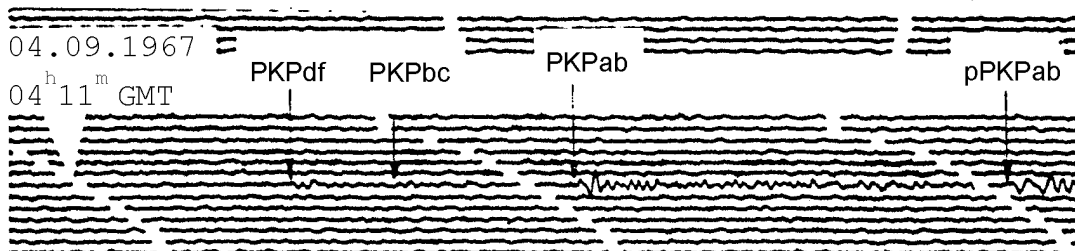


Figure 1 Examples of short-period analog records of stations CLL and MOX of longitudinal core phases in the distance range $135^\circ < D < 160^\circ$. Time scale: 1 mm/s on all records.

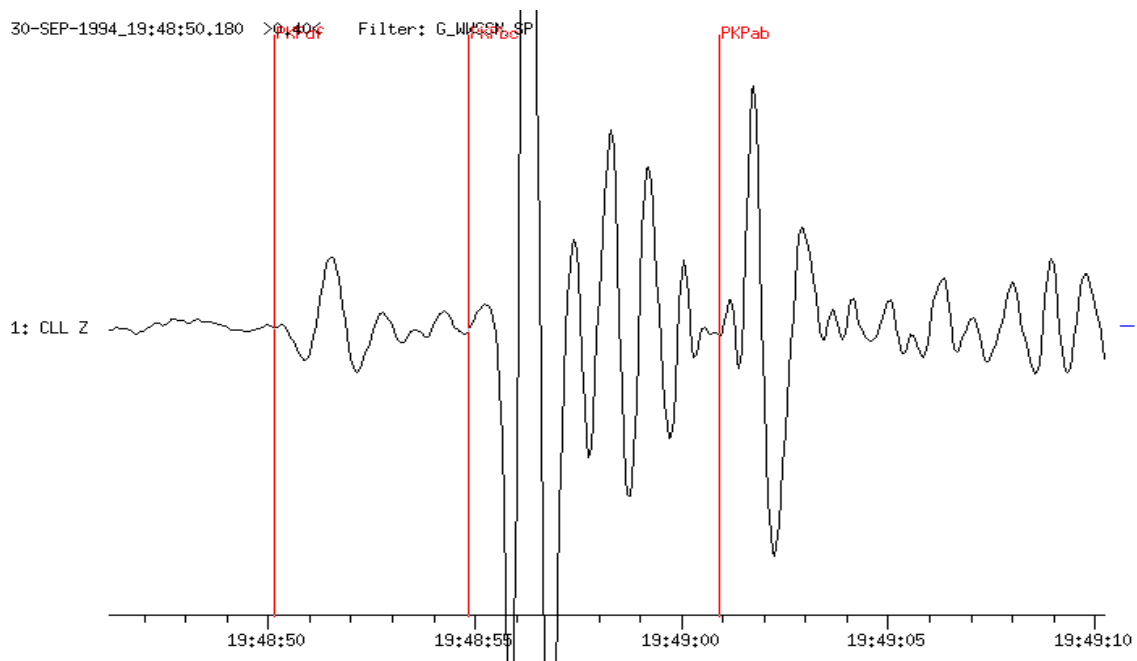
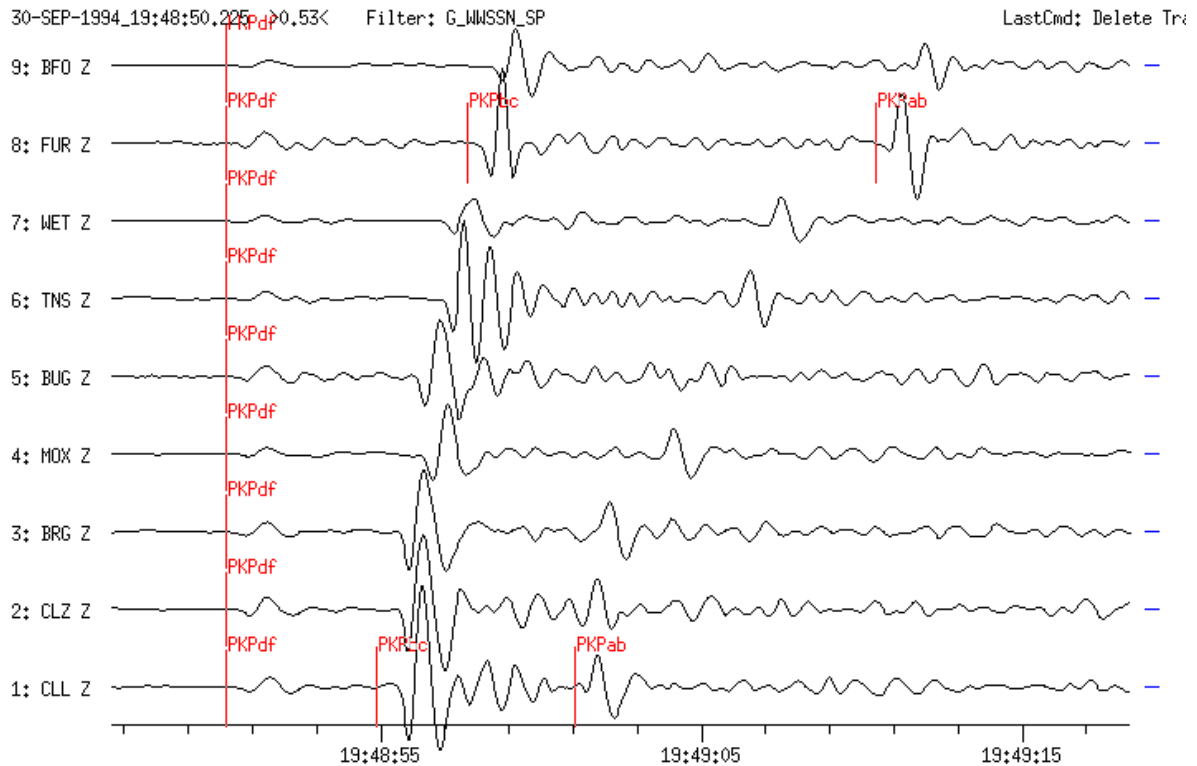


Figure 2 Top: Short-period filtered seismograms (WWSSN_SP simulation) recorded at 9 GRSN stations from a deep earthquake in the Fiji Islands (Sept. 30, 1994, $m_b = 5.1$, $h = 643$ km). All traces are time-shifted and aligned with respect to PKPdf and sorted according to epicentral distance D which is 148.4° for CLL and 152.2° for the most distant station BFO.

Bottom: The same trace of station CLL as above but with enlarged amplitude and time resolution.

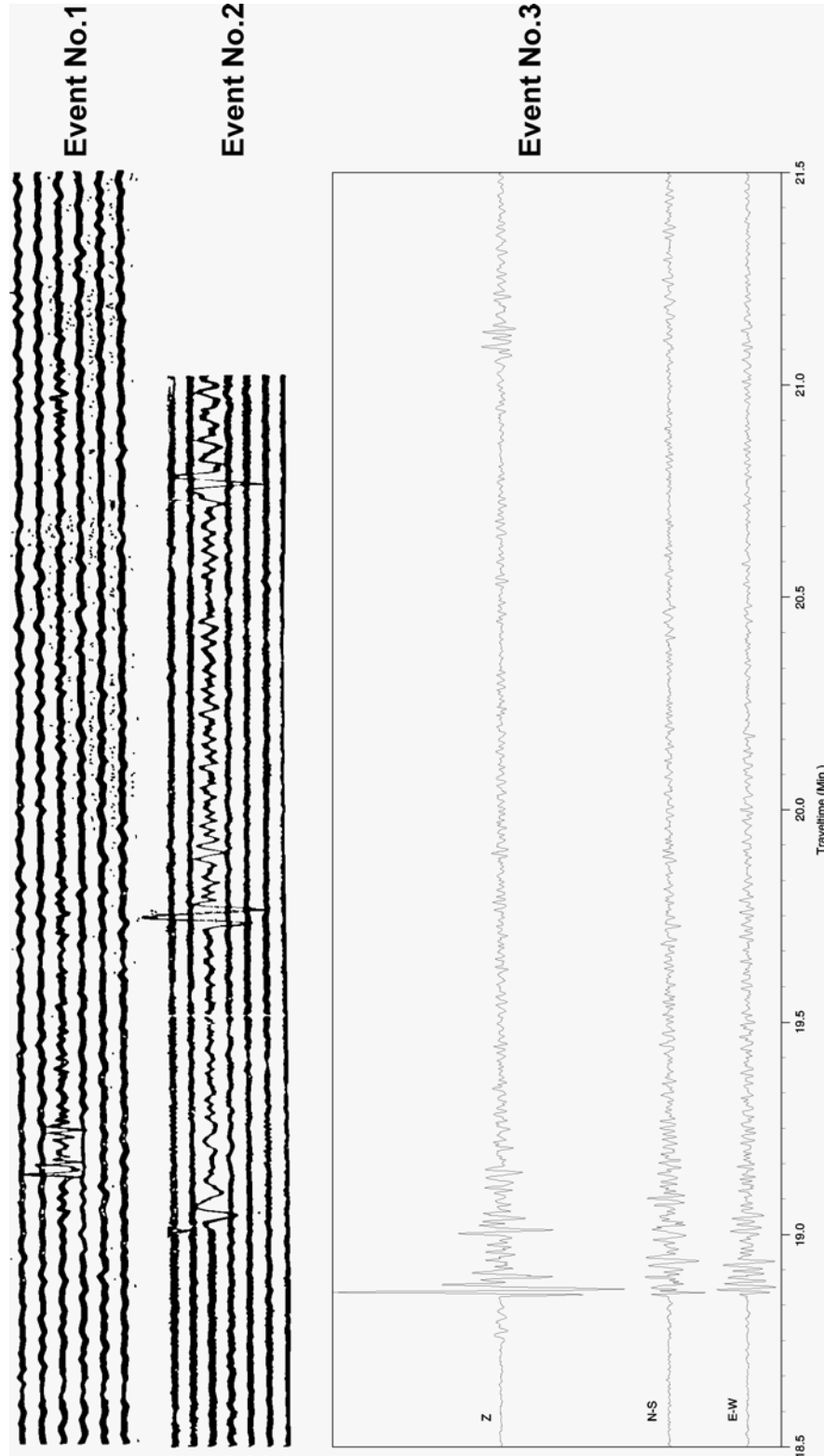
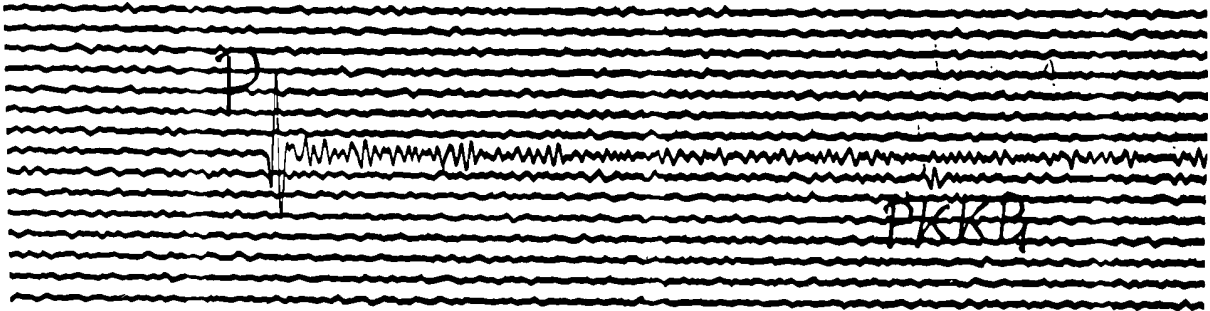
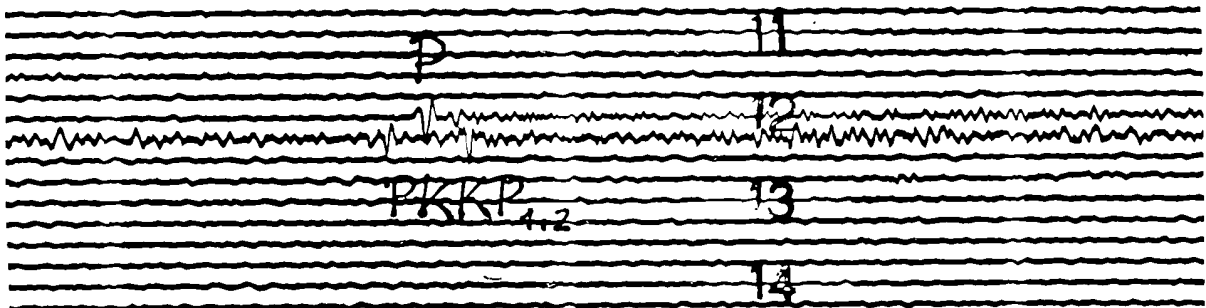


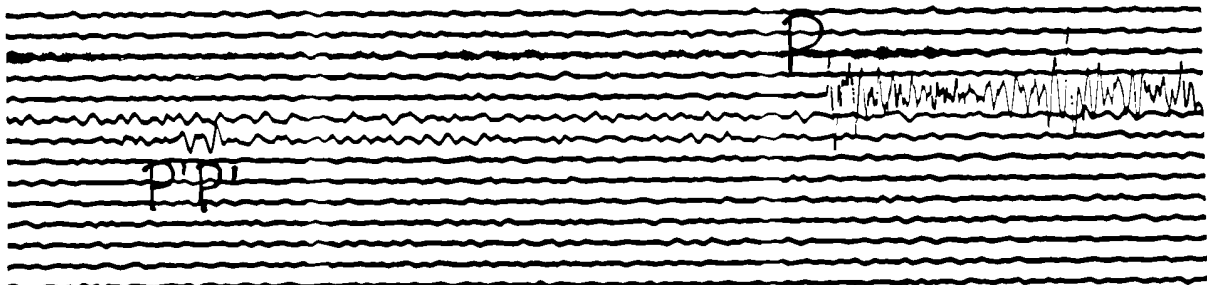
Figure 3 Short-period records of direct longitudinal core phases from three earthquakes. Time scale: 1 mm/s if plotted 1:1.



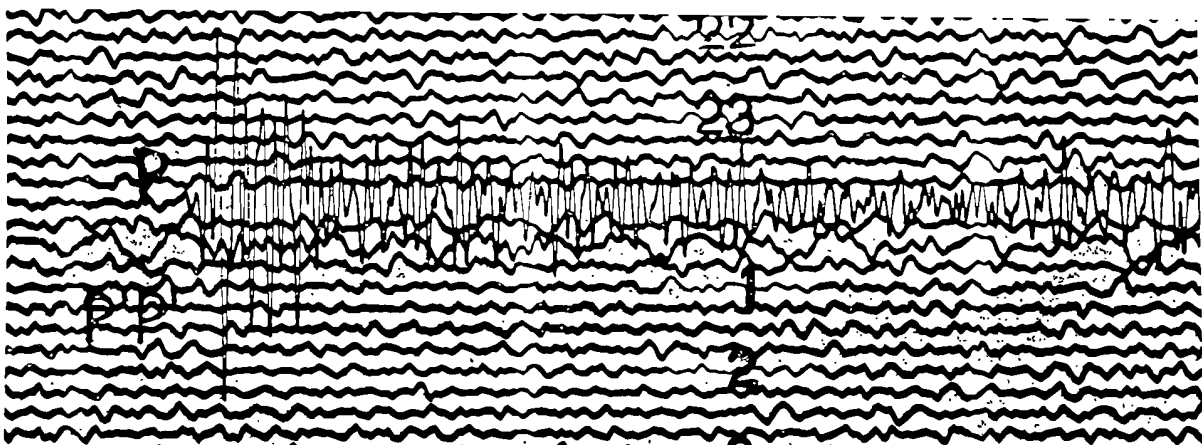
24.08.1995 Mariana Islands: H = 01:55:34.4, D(PLL) = °?, h = 588 km, m_b = 6.0



13.07.1994 Banda Sea: H = 11:45:23.4, D(PLL) = °?, h = 159 km, m_b = 6.5



08.08.1994 Myanmar: H = 21:08:31.7, D(PLL) = °?, h = 122 km, m_b = 6.1



18.02.1996 North of Ascension Island: H = 23:49:27.8, D(PLL) = °?, h = 10 km, m_b = 6.3

Figure 4 Records of station CLL of later reflected longitudinal core phases (PKKP and P'P').

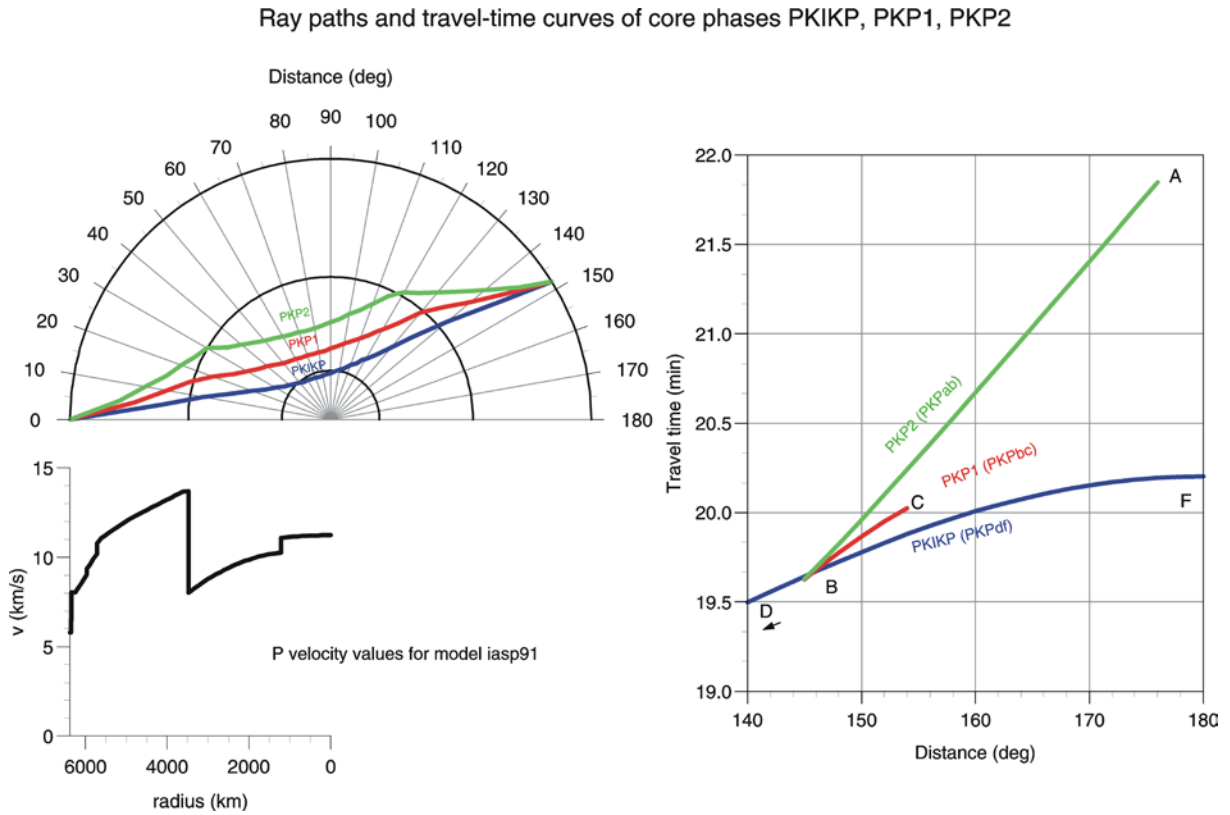


Figure 5 Ray paths and travel-time curves of direct longitudinal core phases for $D > 140^\circ$ according to the velocity model IASP91 (Kennett, 1991).

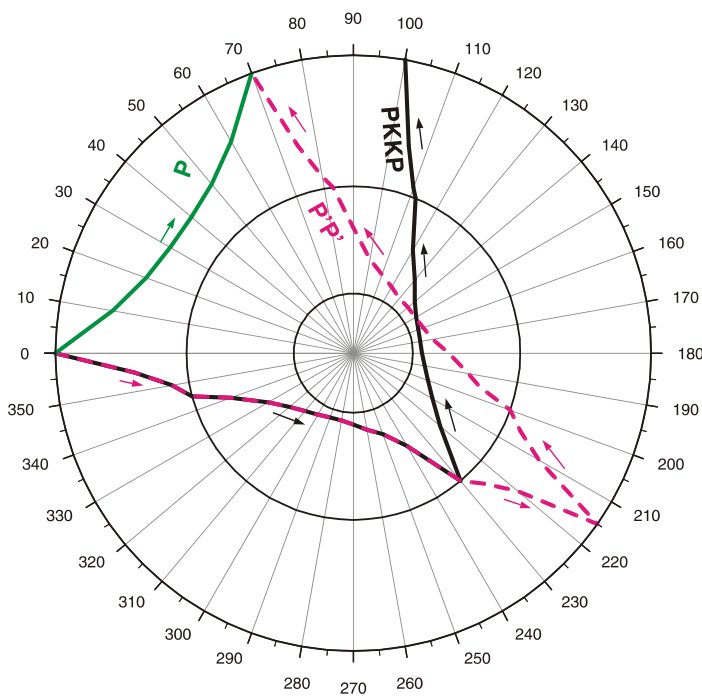


Figure 6 Ray paths of the reflected core phases P'P'(or PKPPKP) and PKKP, respectively.

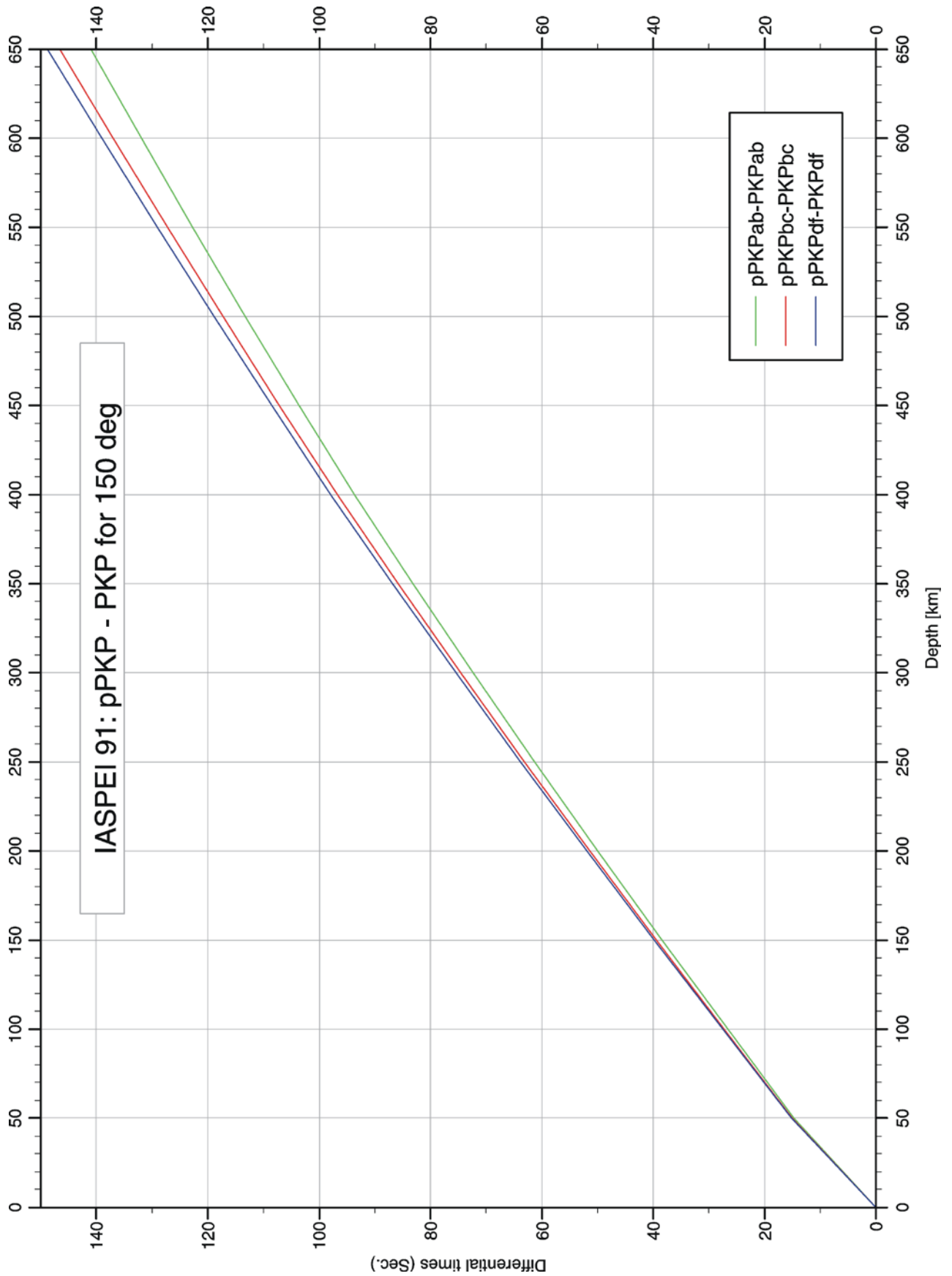


Figure 7 Travel-time differences between the PKP arrivals for the branches ab, bc and df, respectively, and their related depth phases at an epicentral distance of $D = 150^\circ$.

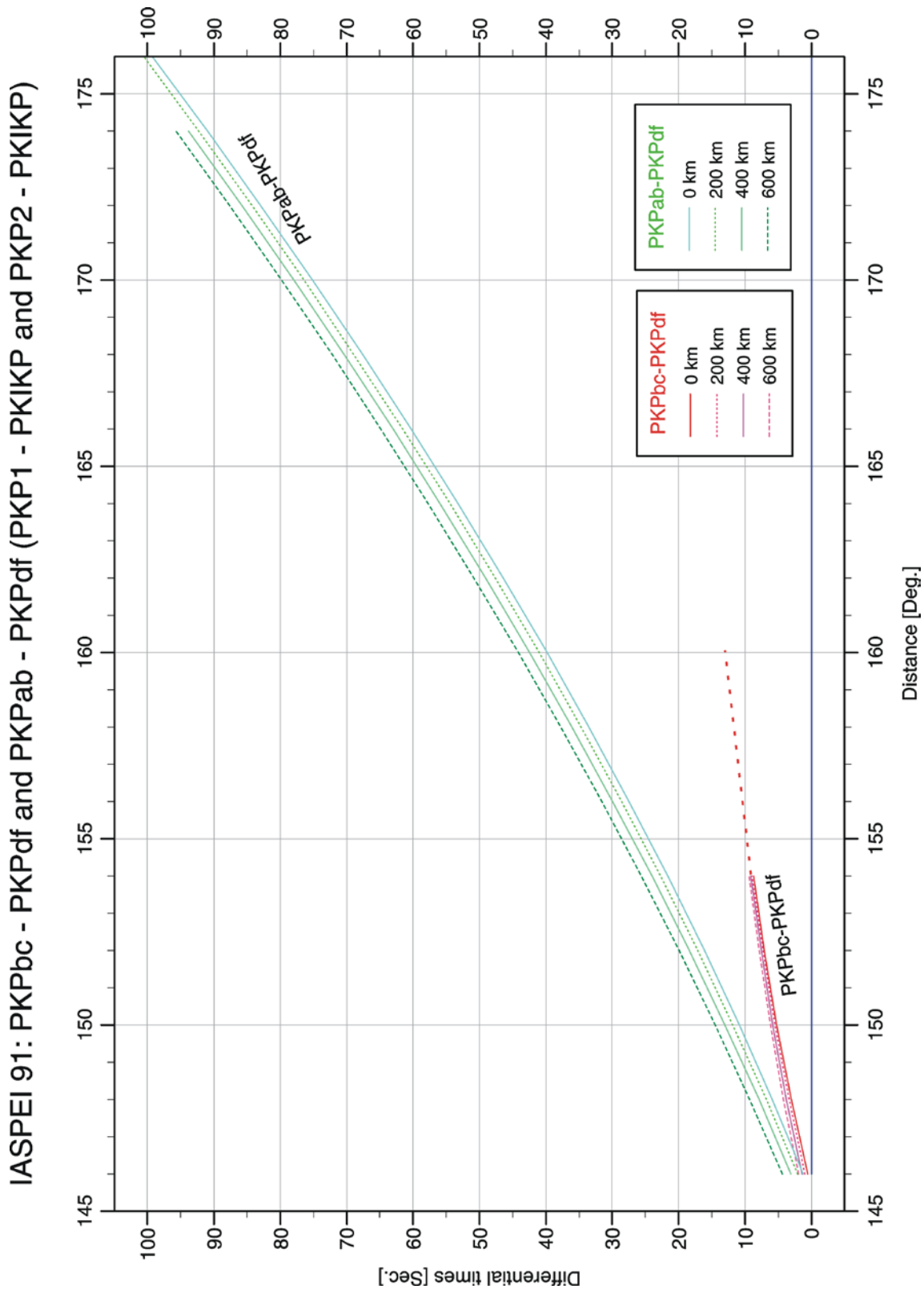


Figure 8 Travel-time differences between the PKPdf first arrival and the later arrivals PKPbc and PKPab, respectively, for different source depths. The dotted continuation of the branch

PKPbc-PKPdf relates to the approximate differential arrival time of the weak phase PKPdif (PKP diffracted around the inner-core boundary).

PKKP - P and PKKP - PKP

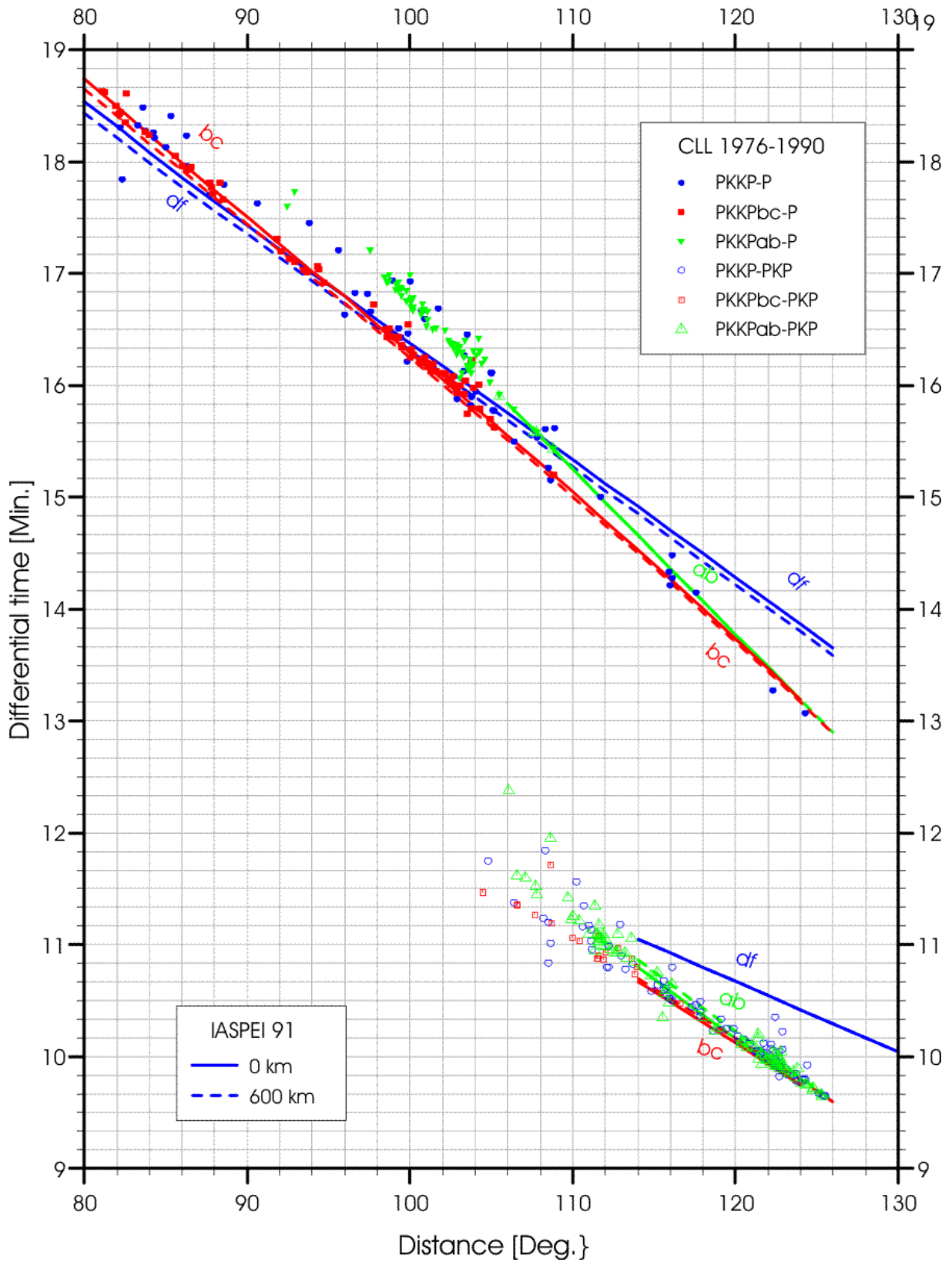


Figure 9 Comprison between theoretical (IASP 91) and observed travel-time differences for PKKP-P and PKKP-PKP at station CLL as a function of epicentral distance and source depth.

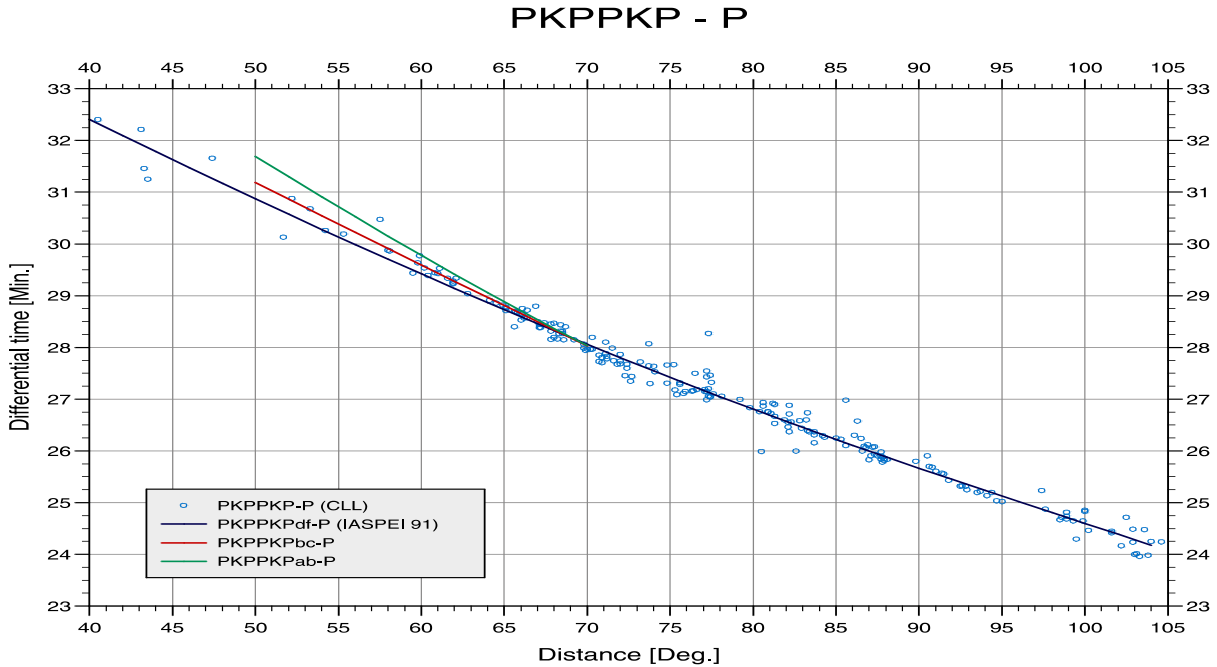


Figure 10 Comparison between theoretical (IASP91) and observed travel-time differences PKPPKP - P at station CLL depending on epicentral distance.

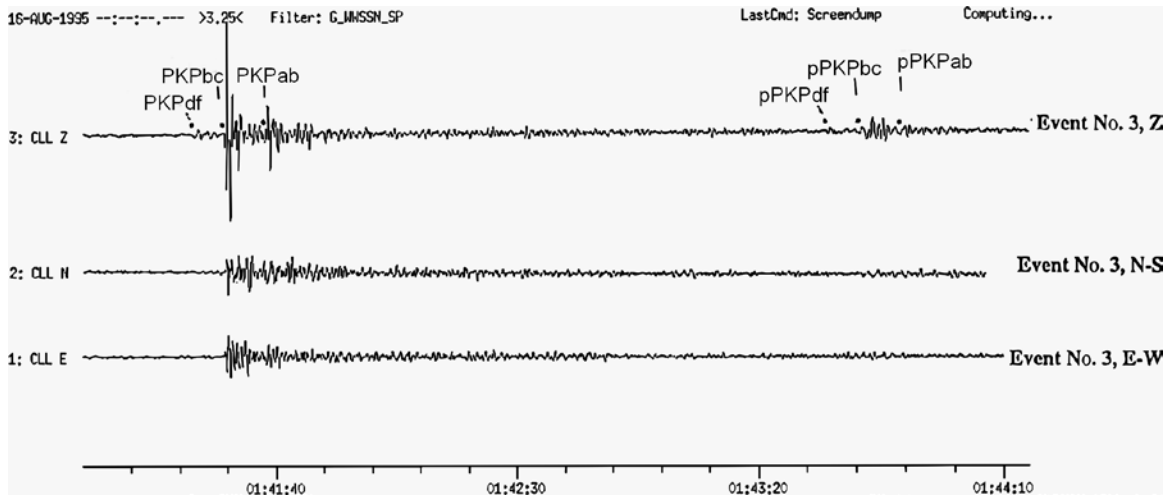


Figure 11 Reproduction of the records of event No. 3 with onsets (dots) marked and names of identified phases given on the vertical component. Only the onset of the depth phase PKPbc can be picked without any doubt. However, when taking the time differences between the three direct phases from the beginning of the record into account one recognizes prior and after pPKPbc changes in the waveforms just at the same time differences as for the primary phases. In the records of earthquakes No. 1 and No. 2 in Figure 3 only the depth phases pPKPbc and pPKPab can be picked at about 119 s and 60 s after PKPbc and PKPab, respectively.

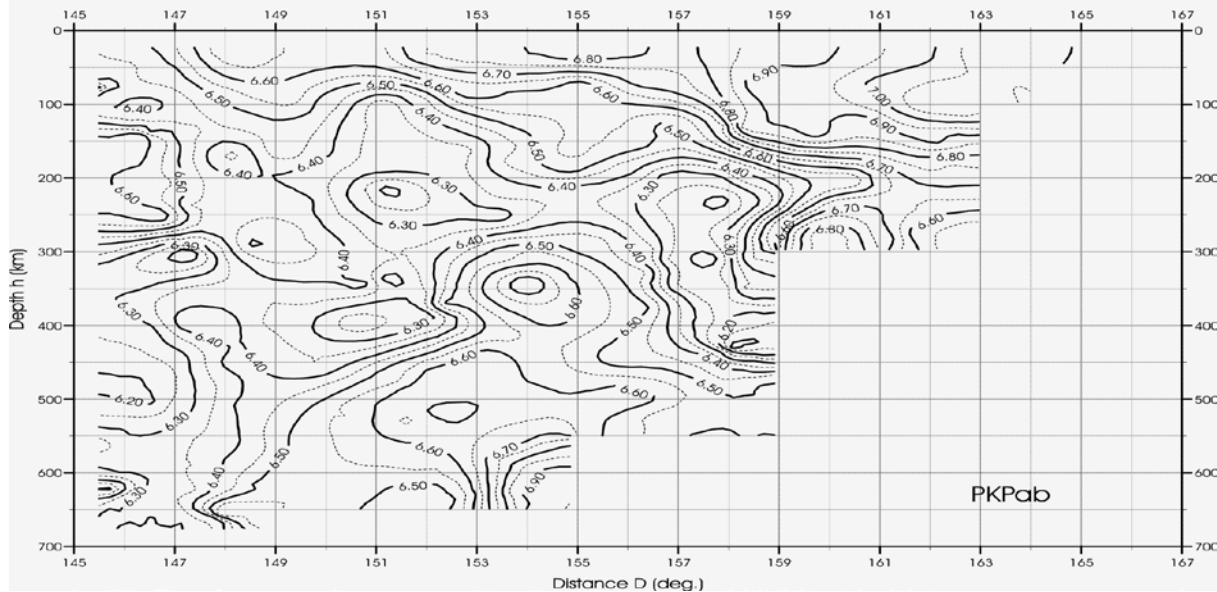
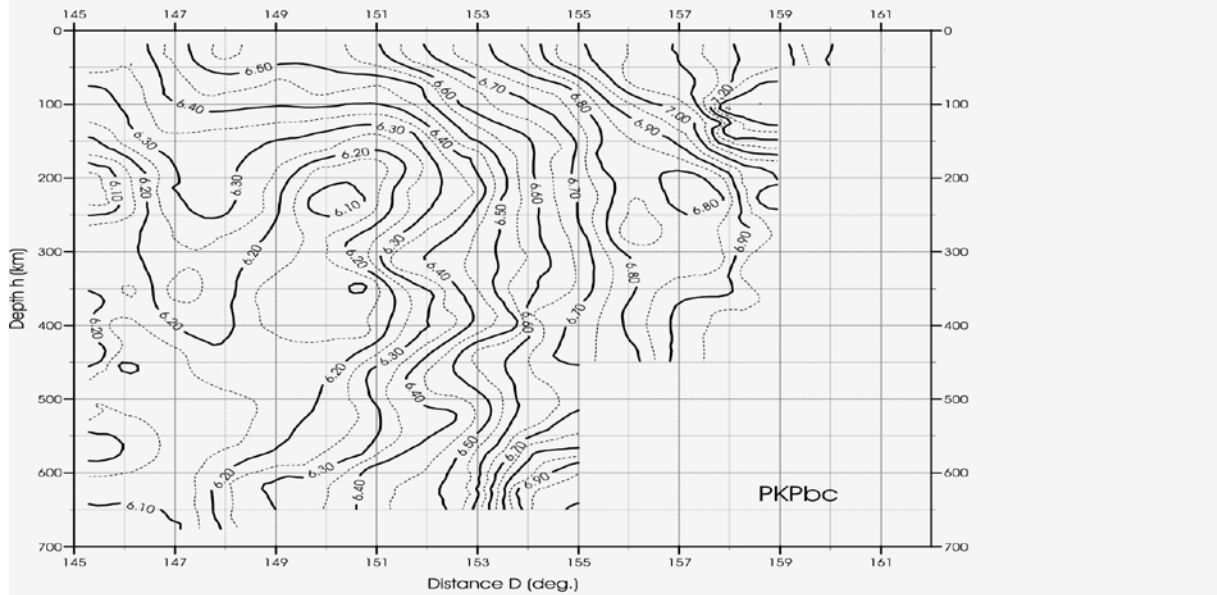
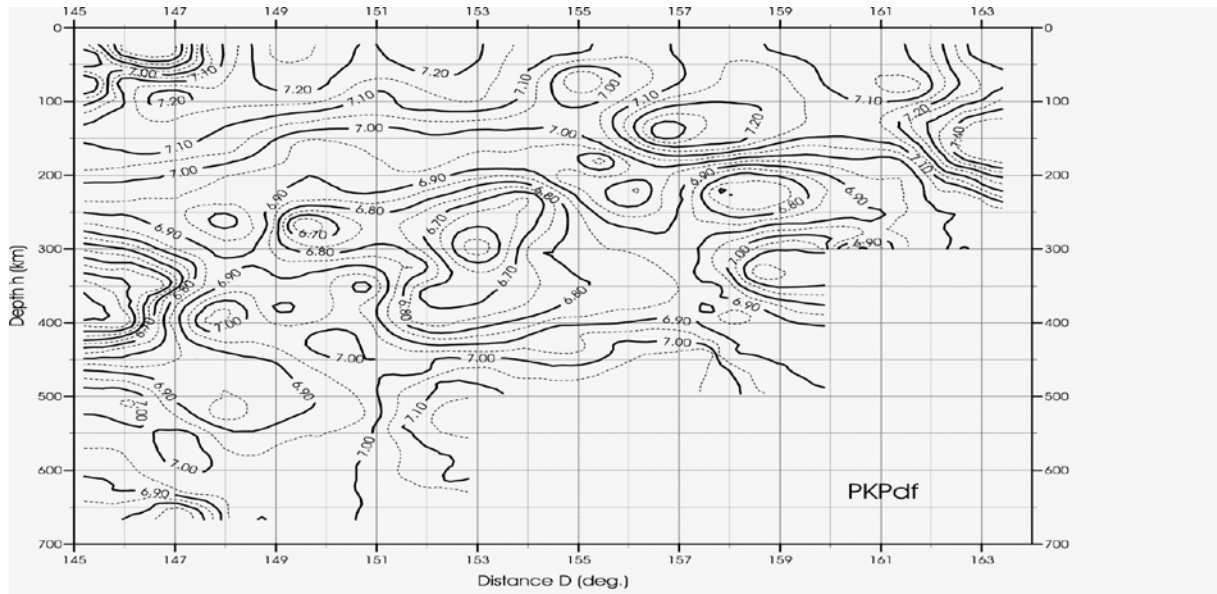


Figure 12 Calibration functions according to S. Wendt for the determination of mb(PKP) for PKIKP = PKPdf, PKP1 = PKPbc and PKP2 = PKPab (see Bormann and Wendt, 1999).

References

- Jeffreys, H., and Bullen, K. E. (1940, 1948, 1958, 1967, and 1970). Seismological Tables. British Association for the Advancement of Science, *Gray Milne Trust*, London, 50 pp.
- Kennett, B. L. N. (Ed.) (1991). IASPEI 1991 Seismological Tables. Research School of Earth Sciences, Australian National University, 167 pp.
- Kennett, B. L. N., and Engdahl, E. R. (1991). Traveltimes for global earthquake location and phase identification. *Geophys. J. Int.*, 105, 429-465.
- Kennett, B. L. N., Engdahl, E. R., and Buland, R. (1995). Constraints on seismic velocities in the Earth from traveltimes. *Geophys. J. Int.*, 122, 108-124.
- Bormann, P., and Wendt, S. (1999). Identification and analysis of longitudinal core phases: Requirements and guidelines. In: Bormann (1999), 346-366.